

## Abstract

Gas Electron Multiplier (GEM) based detectors are widely used in numerous collider experiments and, in particular, at the Budker Institute of Nuclear Physics (BINP). Thus, limits of spatial resolution, achieved by these detectors, are of significant interest. In order to determine the best possible spatial resolution, the simulation of charged particle registration process was accomplished. The simulation of applied detector configurations includes transport of electrons through the detector and tracking of avalanche evolution inside the working volume, as well as obtaining signal distribution on the readout strips. The simulation shows that spatial resolution is definitely less than 50 microns for applied detector configurations. The simulation of electron transport through single GEM and through GEM-cascade showed that an electron cluster is compressed by GEM holes and an effective transverse diffusion is reduced. The experimental part of the work is devoted to the operability tests of the designed detector for the Extracted Beam Facility (EBF-detector) at VEPP-4M collider with orthogonal strips readout with a pitch of 250  $\mu\text{m}$  and the measurements of its characteristics including the dependence of gain on GEM-voltage, the detection efficiency and the spatial resolution.

## Introduction

Charge particle tracking detectors based on Gas Electron Multipliers [1] are used in several projects [2] at the Budker Institute of Nuclear Physics. Firstly, they operate at the Tagging System of the KEDR experiment at the electron-positron collider VEPP-4M since 2010 [3]. Secondly, GEM-based detectors are included to the Photon Tagging System of the DEUTERON facility at VEPP-3 storage ring [4]. The readout in these detectors is provided by straight and inclined strips with a pitch of 500  $\mu\text{m}$ . A new detector for Extracted Beam Facility at VEPP-4M collider [5], having orthogonal strips with a pitch of 250  $\mu\text{m}$ , was assembled and its characteristics were measured.

The present work is aimed to study the limits of spatial resolution of the triple GEM detectors. For this purpose the simulation of different detector configurations in order to find the parameters providing the best spatial resolution was developed. The results of simulations are compared with the measurements performed with the detectors.

## Simulation with GEANT4 and HEED

The simulation study of spatial resolution of the triple-GEM detectors is performed in two stages. At first, primary 1 GeV electrons with momentum perpendicular to the detector plane and randomly distributed initial transverse coordinates in the detector plane are transported through the complete model of the detector (described in GEANT4). After recording of all energy depositions in the drift gap (filled with Ar-CO<sub>2</sub>(25%) gas), the second stage is started that includes introduction of electrons diffusion, gas gain fluctuation, distribution of signal between readout strips, accounting of electronics noise and calculation of the measured track position with Center Of Gravity (COG) method.

The coordinate of the track, passing through the simulated detector is known exactly. This simulation of individual detector aims at optimization purposes and is intended for search of the best possible value of spatial resolution with parameters, providing this value.

The diffusion coefficient, set in the simulation, is of significant interest because standard values, which could be found in the literature, are not fitted for the discussed simulation because the influence of GEM operation should be taken into account. Thus, additional study was provided in order to find the coefficient of effective transverse diffusion (see the next section).

If the central obtained value of effective transverse diffusion 300  $\mu\text{m}/\sqrt{\text{cm}}$  is set to the simulation of detector response, the following results are obtained (Fig. 1). The simulation was provided for two types of readout structure. First, DEUTERON type of readout structure was simulated as a sequence of strips with a pitch of 500  $\mu\text{m}$  and 250  $\mu\text{m}$  width. Exactly three signal strips were accounted in the COG calculation. Second, EBF type of readout structure was simulated as a sequence of strips with a pitch of 250  $\mu\text{m}$  and width 250  $\mu\text{m}$ . Number of strips, accounted in the COG calculation was not limited and determined by the threshold of 3 standard deviation of noise distribution ( $\sigma_{\text{noise}}$ ) on strips.

It was noticed, that essential influence on measured spatial resolution is due to a number of signal strips, involved in the COG calculation. In the experiment with DEUTERON detectors, three strips were implemented in the COG calculation. In case of the EBF-detector strips with signal exceeded  $3 \times \sigma_{\text{noise}}$  were accounted for the coordinate calculation. The results show that algorithm of COG calculation without fixed number of strips works better (resolution is better) for wide range of strip pitch.

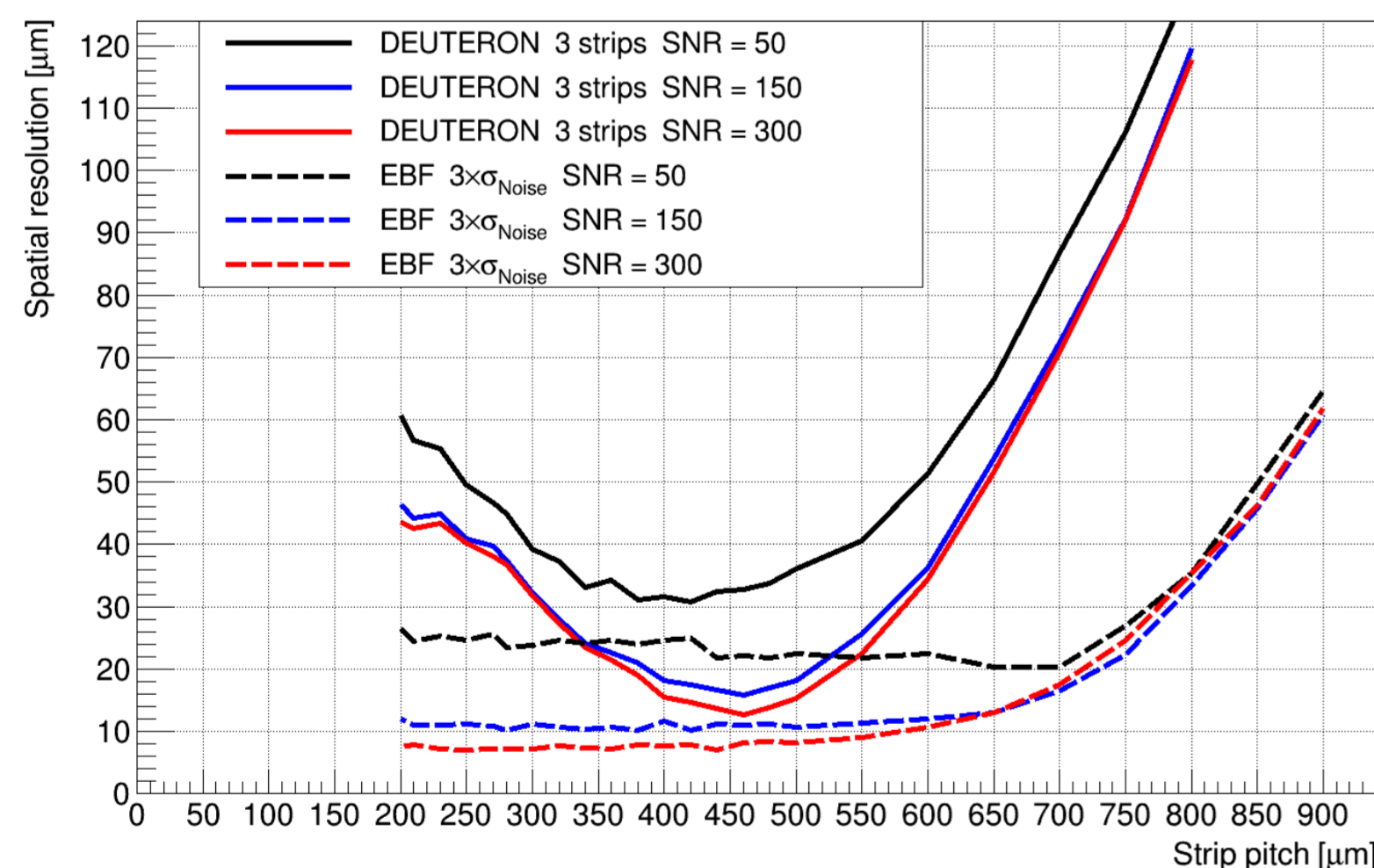


Fig. 1. Triple-GEM detector spatial resolution as a function of strip pitch for the readout structure of DEUTERON and EBF types, obtained in the simulation for different Signal-to-Noise Ratios (SNR) and different algorithms of COG calculations.

## Simulation with ANSYS and Garfield++

In order to provide the detailed simulation for effective transverse diffusion determination, ten thousands events of 1 GeV electron penetration through the drift gap of the detector were generated in HEED program preliminarily (Fig. 2), and thermalized electrons were obtained. Then these electrons were transported (Fig. 3) through 3 cascades of GEMs with Garfield++ program in the presence of electric fields, calculated beforehand in the ANSYS program.

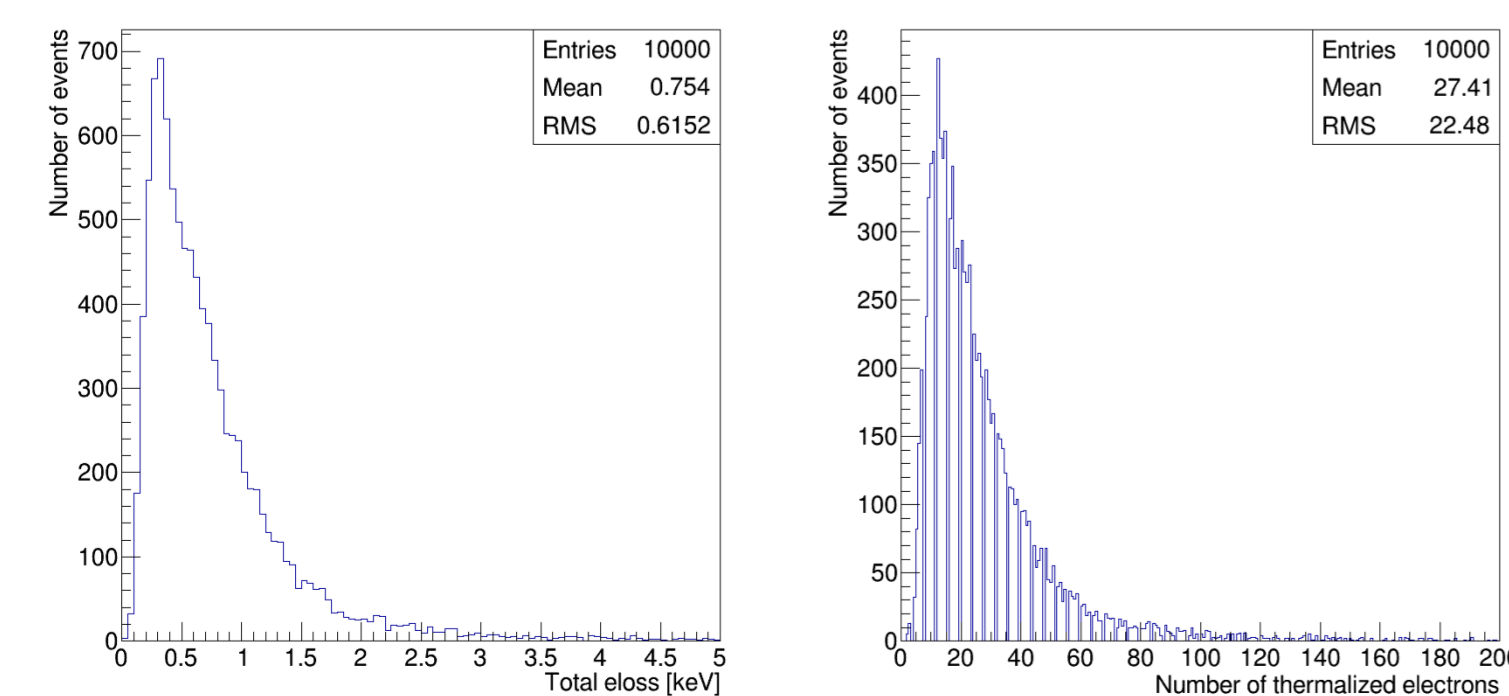


Fig. 2. Total energy loss distribution in events of 1 GeV electron passing through a drift gap (left). Number of thermalized electrons in events (right).

Different relative arrangements of GEM holes were applied in order to determine the range, where effective transverse diffusion could be found. Each thermalized electron in event was transported through the detector and standard deviation of electron distribution on the anode, resulting from one event, was measured. This value, normalized to 1 cm of drift, was assigned as the coefficient of effective transverse diffusion, which could be implemented in the simulation of detector response. The coefficient of effective diffusion for events with different numbers of thermalized electrons is shown in Fig. 4. Averaging values, obtained for different configurations, the coefficient of effective transverse diffusion was estimated as  $300 \pm 20 \mu\text{m}/\sqrt{\text{cm}}$ . The transverse diffusion coefficient for a uniform field of 5 kV/cm, obtained with an analogous method, was found to be  $331 \pm 2 \mu\text{m}/\sqrt{\text{cm}}$ . Hence, GEM operation efficiently compresses transverse size of electron cloud up to 15%.

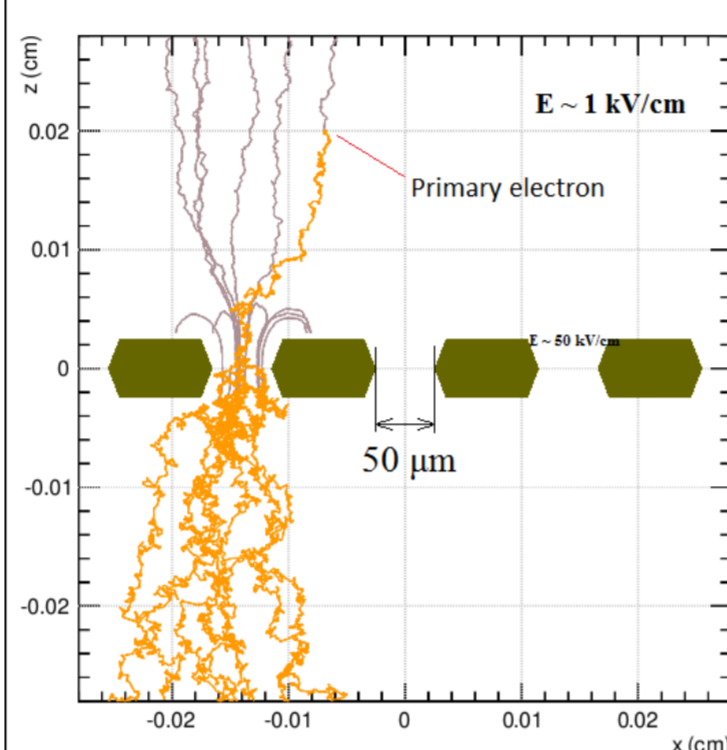


Fig. 3. Development of electron avalanche in the GEM hole and the diffusion of electrons in Ar-CO<sub>2</sub>(25%) (1 atmosphere pressure and 20 °C temperature) under electric field around 1 kV/cm in the gas gaps, simulated in Garfield++.

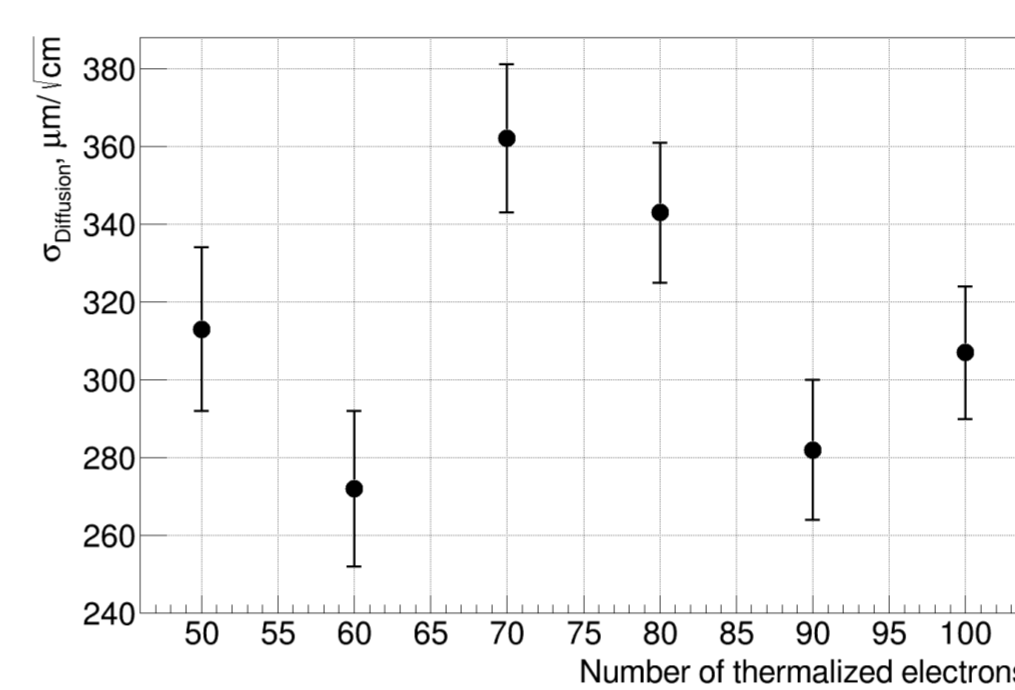


Fig. 4. Coefficient of effective transverse diffusion, calculated for different number of thermalized electrons with fixed arrangement of GEM holes (GEM-2 holes are biased 50  $\mu\text{m}$  left and GEM-3 holes – 20  $\mu\text{m}$  right relatively to GEM-1 holes).

## Detector description

The readout strip structure of the detectors, used for the measurements, is produced on 50  $\mu\text{m}$  thick kapton foil, and all copper layers on GEMs and readout flex (Fig. 4) are reduced as much as possible to decrease the amount of material. Earlier experiments on the measurement of the amount of material demonstrated that expected value of material budget ( $X/X_0$ ) of studied detectors is in the range 0.25% – 0.30%. The readout structure consists of two layers. The strips width of the top layer is 50  $\mu\text{m}$ . Strips of the bottom layer are orthogonal to the top ones with a width of 170  $\mu\text{m}$  and the same pitch 250  $\mu\text{m}$ . The distance between top and bottom layers is 50  $\mu\text{m}$ . The configuration of the readout structure make charge being distributed equivalently between layers.

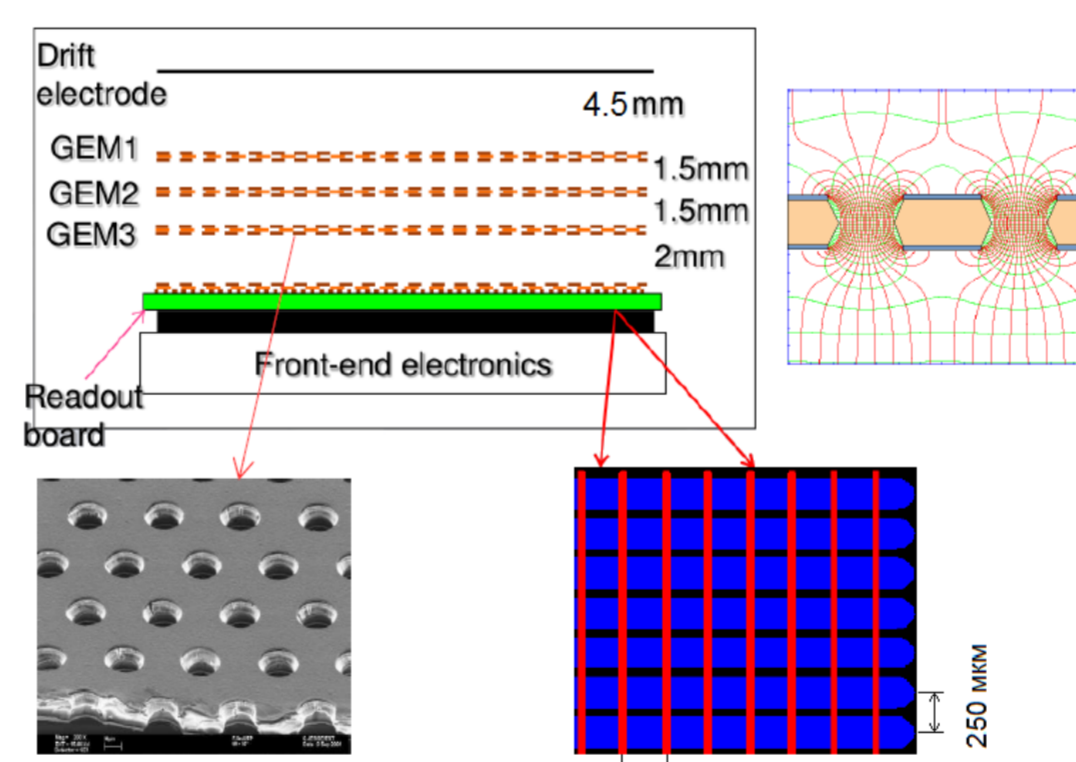


Fig. 4. EBF-detector structure and schematic view of the readout flex design.

## Experimental results

Detector gas gain, detection efficiency and spatial resolution of the EBF-detector were measured with the set-up at the facility of extracted electron beam at VEPP-4M storage ring, shown in Fig. 5. Electron beam with 1 GeV energy was used in the measurements.

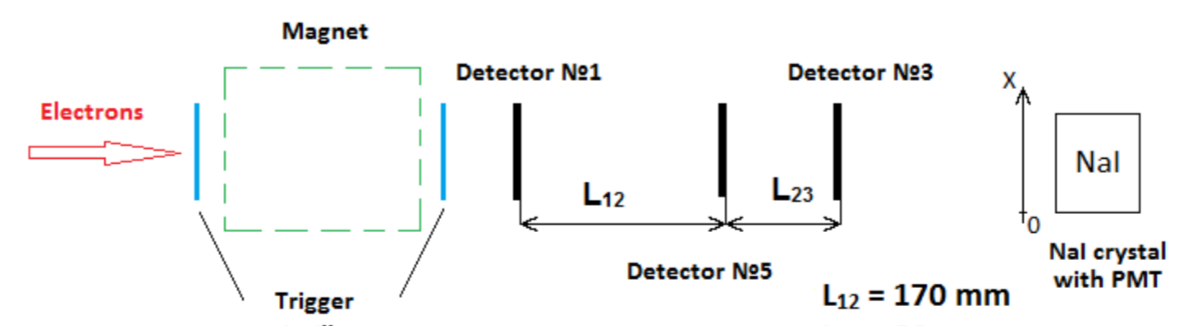


Fig. 5. Schematic view of the experimental set-up. Distances between detectors are  $L_{12} = 170.0 \text{ mm}$ ,  $L_{23} = 80.0 \text{ mm}$ . Two detectors nearest to the central one are used as the tracking detectors.

The same voltage was applied for all three GEMs in cascade. The dependence of the detector gain on single GEM voltage detection efficiency on gain is shown in Fig. 6. The detector works in the proportional regime achieving gain of  $5 \times 10^4$ . Detection efficiency exceeds 99.5% for gain higher than  $3 \times 10^4$ .

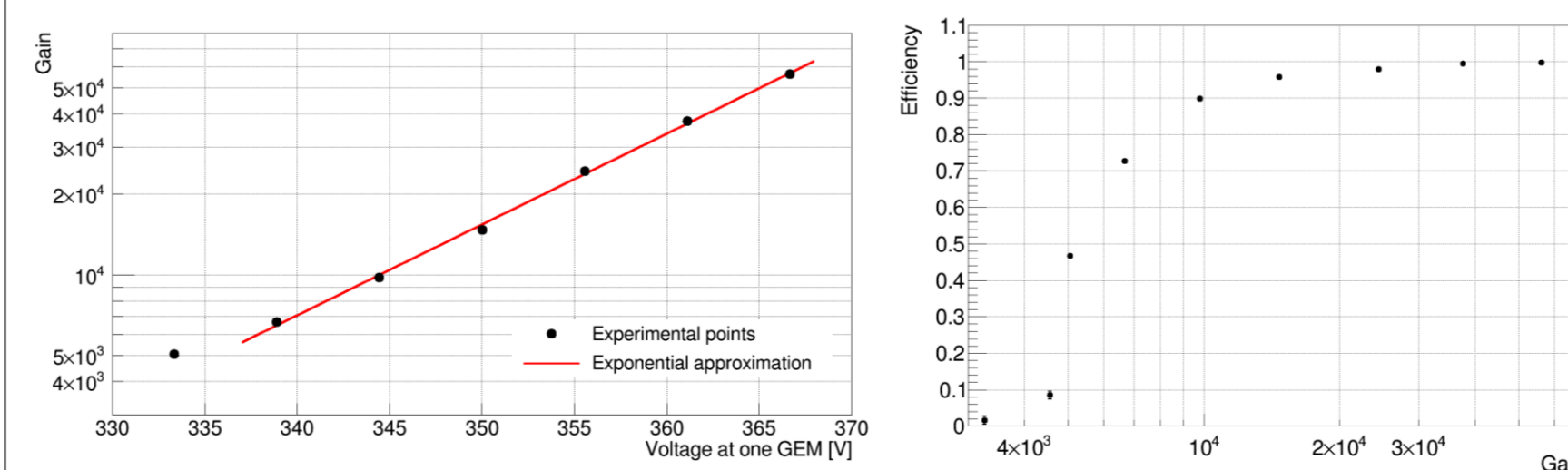


Fig. 6. Dependence of EBF-detector gain on voltage at a single GEM (left) and detection efficiency of the detector as a function of gas gain (right).

In order to minimize systematical errors due to relative rotations between detectors, small regions of the studied detector were investigated. Inside region with best value of spatial resolution scan over track angle was provided. The spatial resolution dependence on track angle is shown in Fig. 7. The contribution of the multiple scattering in the studied detector and the tracking detector resolution was subtracted in order to obtain true resolution of the studied detector. Areas in Fig. 7 show corridors of systematical uncertainties due to non-precise knowledge of material budget ( $X/X_0$ ) of the studied EBF-detector and limited coordinate resolution of tracking detectors ( $\sigma_{\text{tracking}}$ ). The parameters, which were put in the subtracted terms were chosen according to preliminarily accomplished measurements. Top curve in Fig. 8 corresponds to minimal subtraction ( $X/X_0 = 0.25\%$ ,  $\sigma_{\text{tracking}} = 35 \mu\text{m}$ ), bottom curve corresponds to maximum subtraction ( $X/X_0 = 0.30\%$ ,  $\sigma_{\text{tracking}} = 50 \mu\text{m}$ ). Middle curves correspond to intermediate subtractions: ( $X/X_0 = 0.30\%$ ,  $\sigma_{\text{tracking}} = 35 \mu\text{m}$ ) for intermediate top curve and ( $X/X_0 = 0.25\%$ ,  $\sigma_{\text{tracking}} = 50 \mu\text{m}$ ) for intermediate bottom curve. Black line is a quadratic sum of the resolution for orthogonal tracks and track projection to the detector plane  $\sigma = \sqrt{\sigma_0^2 + (L \times \tan(\alpha))^2 / 12}$ , where  $\sigma_0$  is chosen near minimum value of spatial resolution (32  $\mu\text{m}$ ) and  $L$  is the thickness of the drift gap (4.5 mm).

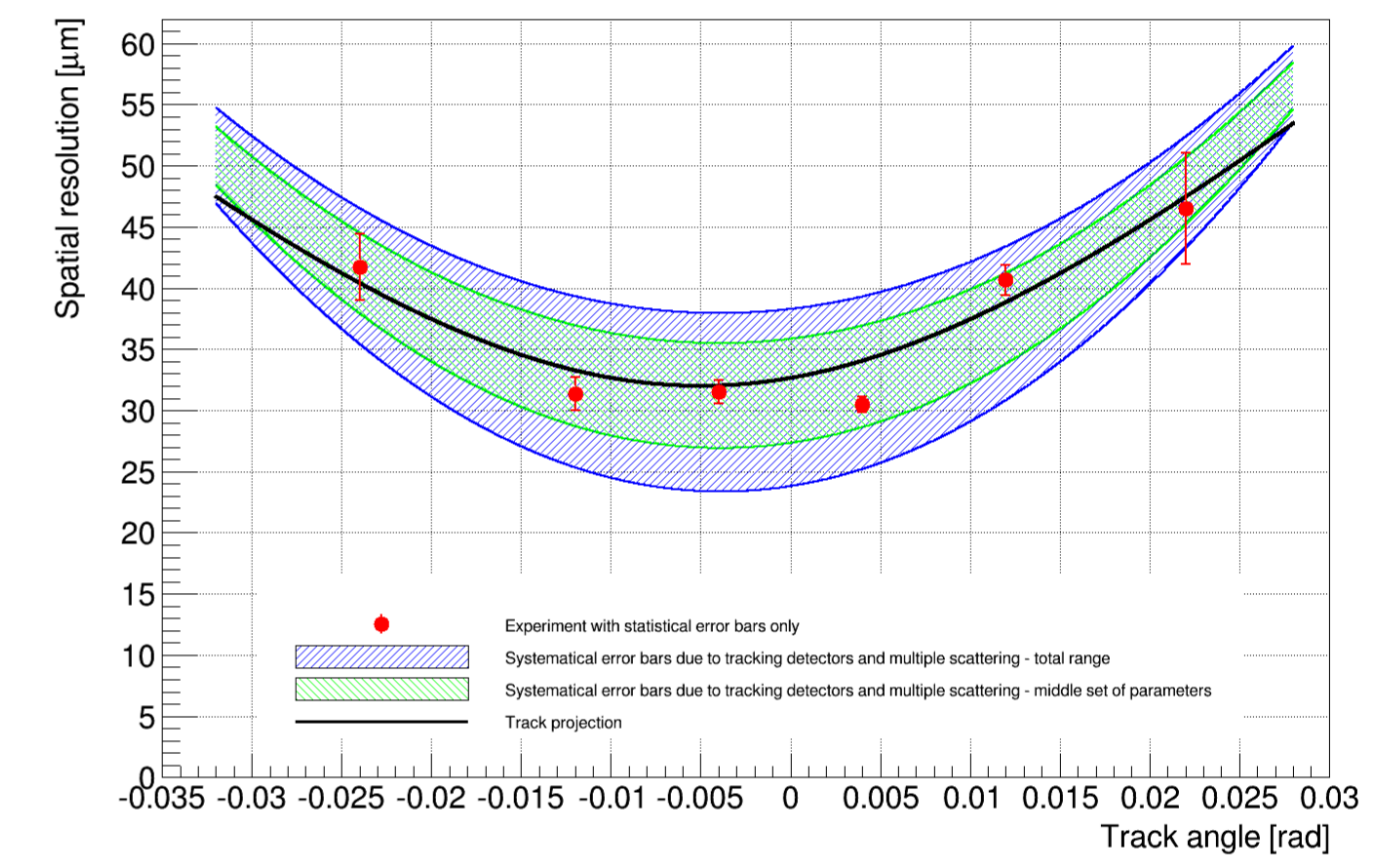


Fig. 7. Spatial resolution as a function of track angle, determined in the experiments with 1 GeV electrons after correction for multiple scattering and limited resolution of the tracking detectors.

The comparison of simulation and experimental results is shown in Fig. 8, where spatial resolutions for orthogonal tracks of two DEUTERON detectors and EBF-detector are pointed.

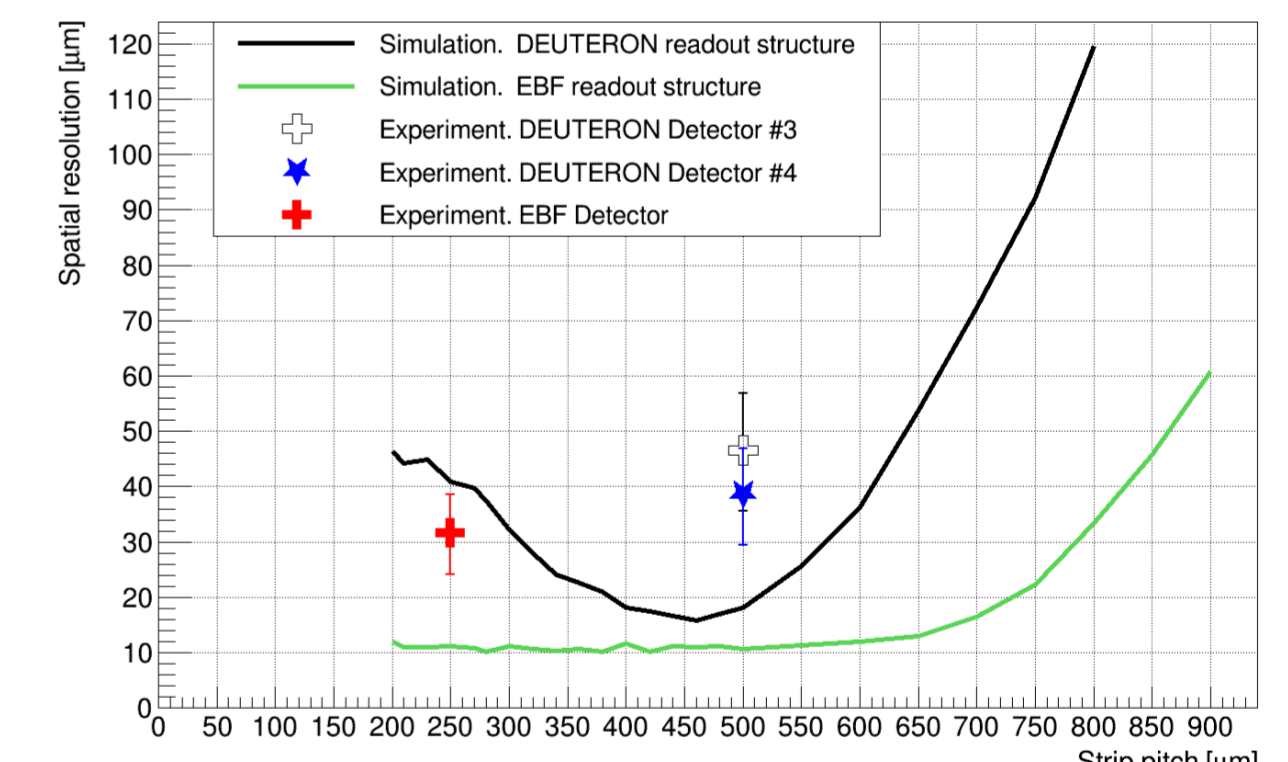


Fig. 8. Triple-GEM detector spatial resolution as a function of strip pitch for the readout structure of DEUTERON and EBF types, obtained in the simulation for SNR = 150, in comparison with the experimental results.

The deviations between simulation and experiment is assumed to be the result of different factor combinations and is the subject of further scrupulous investigation.

## Conclusions

1. The coefficient of effective transverse diffusion, obtained in the detailed simulation of electron transport in the detector is  $300 \pm 20 \mu\text{m}/\sqrt{\text{cm}}$ .
2. The effect of electron cloud compression up to 15% due to GEM operation in comparison with uniform electric field was observed.
3. The simulation of detector response shows essential influence of COG calculation on the counted spatial resolution. At the same time, physical minimum of spatial resolution of 10 – 15  $\mu\text{m}$  level is determined by delta-electron space distribution.
4. Detector for extracted beam facility with 250  $\mu\text{m}$  strip pitch (EBF-detector) demonstrates stable operation with gas gain up to  $5 \times 10^4$  and the detection efficiency exceeding 99% for standard proportional operation regime.
5. Spatial resolution of EBF-detector is measured as

$$\sigma_{\text{EBF-detector}} = 31.5 \pm 0.9 \text{ (stat.) } \pm 6.9 \text{ (syst.) } \mu\text{m}.$$

The angular dependence of spatial resolution is in the agreement with the expectations.

## References:

1. F. Sauli, GEM: A new concept for electron amplification in gas detectors, Nucl. Instrum. Meth. A386 (1997) 531.
2. L. I. Shekhtman et al., Development of high resolution tracking detectors with Gas Electron Multipliers, 2014 JINST 9 C08017.
3. V. M. Aulchenko et al., Operation of the triple-GEM detectors in the tagging system of the KEDR experiment on the VEPP-4M collider, 2011 JINST 6 P07001.
4. V. N. Kudryavtsev et al., The development of high resolution coordinate detectors for the DEUTERON facility, 2014 JINST 9 C09024.
5. G. N. Abramov et al., Extracted electron and gamma beams in BINP, 2014 JINST 9 C08022.